

# Synthesis and Preliminary Evaluation of 18-<sup>18</sup>F-Fluoro-4-Thia-Oleate as a PET Probe of Fatty Acid Oxidation

Timothy R. DeGrado<sup>1</sup>, Falguni Bhattacharyya<sup>2</sup>, Mukesh K. Pandey<sup>1</sup>, Anthony P. Belanger<sup>1</sup>, and Shuyan Wang<sup>1</sup>

<sup>1</sup>Department of Radiology, Brigham and Women's Hospital, Harvard Medical School, Boston, Massachusetts; and <sup>2</sup>Imaging Probe Development Center, National Institutes of Health, Bethesda, Maryland

Fatty acid oxidation (FAO) is a major energy-providing process with important implications in cardiovascular, oncologic, neurologic, and metabolic diseases. A novel 4-thia oleate analog, 18-<sup>18</sup>F-fluoro-4-thia-oleate (<sup>18</sup>F-FTO), was evaluated in relationship to the previously developed palmitate analog 16-<sup>18</sup>F-fluoro-4-thia-palmitate (<sup>18</sup>F-FTP) as an FAO probe. **Methods:** <sup>18</sup>F-FTO was synthesized from a corresponding bromoester. Biodistribution and metabolite analysis studies were performed in rats. Preliminary small-animal PET studies were performed with <sup>18</sup>F-FTO and <sup>18</sup>F-FTP in rats. **Results:** A practical synthesis of <sup>18</sup>F-FTO was developed, providing a radiotracer of high radiochemical purity (>99%). In fasted rats, myocardial uptake of <sup>18</sup>F-FTO (0.70 ± 0.30% dose kg [body mass]/g [tissue mass]) was similar to that of <sup>18</sup>F-FTP at 30 min after injection. At 2 h, myocardial uptake of <sup>18</sup>F-FTO was maintained, whereas <sup>18</sup>F-FTP uptake in the heart was 82% reduced. Similar to <sup>18</sup>F-FTP, <sup>18</sup>F-FTO uptake by the heart was approximately 80% reduced at 30 min by pretreatment of rats with the CPT-1 inhibitor etomoxir. Folch-type extraction analyses showed 70–90% protein-bound fractions in the heart, liver, and skeletal muscle, consistent with efficient trafficking of <sup>18</sup>F-FTO to the mitochondrion with subsequent metabolism to protein-bound species. Preliminary small-animal PET studies showed rapid blood clearance and avid extraction of <sup>18</sup>F-FTO and of <sup>18</sup>F-FTP into the heart and liver. Images of <sup>18</sup>F-FTO accumulation in the rat myocardium were clearly superior to those of <sup>18</sup>F-FTP. **Conclusion:** <sup>18</sup>F-FTO is shown to be a promising metabolically trapped FAO probe that warrants further evaluation.

**Key Words:** fatty acid oxidation; PET; myocardial metabolism

**J Nucl Med 2010; 51:1310–1317**

DOI: 10.2967/jnumed.109.074245

**T**he oxidation of long-chain fatty acids is the major aerobic, energy-producing process in the heart, liver, and skeletal muscle. Abnormalities of fatty acid oxidation (FAO) are associated with a variety of diseases, including

ischemic heart disease (1), heart failure (2), cardiomyopathy (3), oncology (4), neurodegeneration (5), alcoholism (6), nonalcoholic fatty liver (7), obesity or metabolic syndrome (8–10), and diabetes (8,11).

Over the last 20 y, our laboratory has investigated radiolabeled thia-substituted long-chain fatty acid analogs as metabolically trapped probes of myocardial FAO (12–17). The first-generation molecule 14-<sup>18</sup>F-fluoro-6-thia-heptadecanoic acid (<sup>18</sup>F-FTHA) was a 6-thia analog that showed excellent myocardial imaging properties but lacked specificity for mitochondrial FAO in certain conditions such as oxygen insufficiency (14,15). Accumulation of <sup>18</sup>F-FTHA in the liver and skeletal muscle was largely in complex lipid pools and therefore not useful for the indication of mitochondrial FAO in those tissues (16). The second-generation FAO probe 16-<sup>18</sup>F-fluoro-4-thia-palmitate (<sup>18</sup>F-FTP), a 4-thia fatty acid analog, improved on <sup>18</sup>F-FTHA by increasing specificity to myocardial FAO, particularly in response to hypoxia (12,14). However, myocardial retention of <sup>18</sup>F-FTP was suboptimal, and metabolic trapping in the liver was not specific to mitochondrial function (14).

Oleate is one of the most prevalent long-chain fatty acids in human plasma (17,18) and, like palmitate, is used as an energy substrate or incorporated into various complex lipids for storage or as cellular structural components. Although oleate and palmitate have been shown to be similarly taken up and oxidized in human myocardium (18), their use in the whole body and skeletal muscle in humans has shown some notable differences (19–22). Because dietary oleate (18:1) is preferentially oxidized relative to palmitate (16:0) and stearate (18:0) (22), we anticipated that an oleic acid analog of <sup>18</sup>F-FTP might show a higher specificity for mitochondrial FAO than <sup>18</sup>F-FTP itself. Therefore, we synthesized and preliminarily evaluated in rats the 4-thia substituted oleate analog 18-<sup>18</sup>F-fluoro-4-thia-oleate (<sup>18</sup>F-FTO) (1) as a novel PET probe of FAO (Fig. 1). Results of biodistribution and small-animal PET studies were compared with those for the previously developed 4-thia-substituted palmitate analog <sup>18</sup>F-FTP, showing enhanced myocardial imaging characteristics and increased specificity for evaluation of FAO rates in vivo.

Received Dec. 22, 2009; revision accepted Apr. 8, 2010.

For correspondence or reprints contact: Timothy R. DeGrado, Department of Radiology, Brigham and Women's Hospital, Harvard Medical School, 75 Francis St., Boston, MA 02115.

E-mail: tdegrado@partners.org

COPYRIGHT © 2010 by the Society of Nuclear Medicine, Inc.



## Biodistribution Studies in Rats

Female Sprague–Dawley rats (165–215 g; Charles River) were fasted overnight or fed ad libitum. The rats were anesthetized with isoflurane (3.5% induction, 1.5% maintenance). The  $^{18}\text{F}$ -labeled radiotracer (0.7–1.4 MBq) was injected into the tail vein. The heart, liver, lung, blood, kidney, bone (femur), brain, and skeletal muscle were procured after a prescribed time. The tissues were counted for  $^{18}\text{F}$  radioactivity and weighed. Radiotracer uptake was calculated as:

$$\text{Uptake (\% dose kg/g)} = \frac{\text{CPM (tissue)} \times \text{body weight (kg)} \times 100}{\text{tissue weight (g)} \times \text{CPM (dose)}}, \quad \text{Eq. 1}$$

where CPM is counts per minute.

In 1 group of fasted rats, the CPT-I inhibitor etomoxir (40 mg/kg; Sigma-Aldrich) was administered intraperitoneally 2 h before  $^{18}\text{F}$ -FTO injection. Crude analysis of the nature of the metabolites in the heart, liver, and muscle was performed by a Folch-type extraction procedure. Approximately 0.5 g of tissue was excised and thoroughly homogenized and sonicated (20 s) in 7 mL of chloroform/methanol (2:1) at 0°C. Urea (40%, 1.75 mL) and 5% sulfuric acid (1.75 mL) were added, and the mixture was sonicated for an additional 20 s. After centrifugation for 10 min at 1,800g, aqueous, organic, and protein interphase (pellet) fractions were separated and counted for  $^{18}\text{F}$  radioactivity.

## Small-Animal PET/CT Studies in Rats

Two female Sprague–Dawley rats (167–172 g) were fasted overnight. The rats were anesthetized with isoflurane (3.5% induction, 1.5% maintenance). An eXplore Vista CT scanner (GE Healthcare) was used. Before the radiotracer imaging study, a whole-body CT scan was obtained. This scan was used for anatomic visualization and attenuation correction of the emission data.  $^{18}\text{F}$ -FTO and  $^{18}\text{F}$ -FTP were studied in 2 different rats to allow biodistribution studies to be performed after the PET scan. The  $^{18}\text{F}$ -labeled radiotracer (9–11 MBq) was injected into the tail vein, and the emission data were collected in dynamic acquisition for 50 min over the upper thorax, followed by a static whole-body scan from 55 to 115 min after injection. The dynamic images were analyzed to give time–activity curves of the left-ventricular myocardium, blood pool, lung, liver, and bone (rib) at the following consecutive intervals:  $6 \times 10$ ,  $4 \times 30$ ,  $5 \times 60$ , and  $8 \times 300$  s. The time–activity curves were expressed as the commonly used standardized uptake value, which is the PET-measured radioactivity concentration ( $C_t$ ) normalized to body weight and injected dose:

$$\text{Standardized uptake value} = \frac{C_t (\text{kBq/cm}^3) \times \text{body weight (g)}}{\text{dose (kBq)}}. \quad \text{Eq. 2}$$

## Statistical Analyses

All results were expressed as the mean  $\pm$  SD. Comparison of the means was made using a 2-tailed Student *t* test. The acceptable level of significance was set at a *P* value of less than 0.05.

## RESULTS

### Synthesis of $^{18}\text{F}$ -FTO (1)

Figure 2 shows the synthetic scheme. To make (Z)-18-fluoro-4-thia-octadec-9-enoic acid (11) (FTO), 1-bromononanol

was converted to 2-(9-bromononyloxy)tetrahydro-2H-pyran (2), which on subsequent reaction with triphenylphosphine gave [9-((tetrahydro-2H-pyran-2-yl)oxy)nonyl]triphenylphosphonium bromide (3) as an ylide for the Wittig reaction. The ylide precursor was treated with 5-(tert-butylidimethylsilyloxy) pentanal, giving (Z)-tert-butylidimethyl(14-(tetrahydro-2H-pyran-2-yloxy)tetradec-5-enyloxy)silane (4). The formation of compound 4 was characterized by the presence of olefinic protons at  $\delta$  5.38–5.32 (m, 2H) and carbons at  $\delta$  130.1, 129.6 in their nuclear magnetic resonance spectra. Compound 4 was further treated with tetrabutyl ammonium fluoride in tetrahydrofuran to deprotect the hydroxyl group. On iodination, hydroxyl analog 5 gave compound 6. Methyl 3-mercaptopropanoate was then treated with compound 6 in tetrahydrofuran using sodium hydride to obtain (Z)-methyl 18-(tetrahydro-2H-pyran-2'-yloxy)-4-thia-octadec-9-enoate (7). The tetrahydropyran group in compound 7 was removed using *p*-toluenesulfonic acid in methanol. The obtained hydroxyl analog (8) was further reacted with tosyl chloride to obtain the corresponding tosyl ester (9), which on reaction with lithium bromide gave (Z)-methyl 18-bromo-4-thia-octadec-9-enoate (10), the optimal bromoester precursor for radiofluorination. The cold fluorinated standard (11) was also synthesized from compound 9. The intermediates and the final precursor were characterized by detailed spectroscopic analyses.

Radiofluorination of the bromoester (10) proceeded efficiently, with more than 70% incorporation of  $^{18}\text{F}$ -fluoride into the corresponding  $^{18}\text{F}$ -fluoroester. Hydrolysis of the methylester group by the addition of 0.2N KOH and continued heating was quantitative, and overall radiochemical yields after preparative HPLC isolation were in the 20–30% uncorrected range and not further optimized. Radiochemical purity of the product (1) by radio-HPLC or radio-thin-layer chromatography was more than 99%. The product was effectively formulated in 0.5–1.0% bovine serum albumin solution in saline and sterile-filtered before being administered to rats. Likewise, the palmitate analog,  $^{18}\text{F}$ -FTP, was synthesized by a similar approach as previously described (14).

## Biodistribution Studies in Rats

Table 1 shows the biodistribution of  $^{18}\text{F}$  radioactivity in rats after intravenous administration of  $^{18}\text{F}$ -FTO at 30 and 120 min after injection. In both fasted and fed rats at 30 min, the highest uptake was seen in the liver, followed by the heart, kidney, and other organs. The only difference in biodistribution between fasted and fed rats was a 29% lower uptake in the livers of fed animals. Clearance from the liver was seen between 30 and 120 min in fasted animals, whereas heart uptake was maintained at 0.7–0.8% dose kg (body mass)/g (tissue mass). Pretreatment of fasted rats with the CPT-I inhibitor etomoxir resulted in an 80% reduction in myocardial uptake of  $^{18}\text{F}$ -FTO ( $P < 0.02$ ), consistent with the previously reported decrease of  $^{18}\text{F}$ -FTP uptake by rat heart under similar experimental conditions (14). Bone uptake of

**TABLE 1. Uptake (% Dose kg/g) of <sup>18</sup>F-FTO and <sup>18</sup>F-FTP in Sprague-Dawley Rats**

Organ/tissue	<sup>18</sup> F-FTO uptake			<sup>18</sup> F-FTP uptake in control fasted rats	
	Control fasted rats				
	Control fed rats at 30 min (n = 6)	At 30 min (n = 6)	Etomoxir*-treated fasted rats at 30 min (n = 4)	At 30 min (n = 6)	At 120 min (n = 6)
Blood	0.0326 ± 0.0035	0.0442 ± 0.0122	0.0659 ± 0.0324	0.070 ± 0.059	0.0106 ± 0.0028†
Heart	0.697 ± 0.193	0.703 ± 0.302	0.138 ± 0.078‡	0.589 ± 0.257	0.107 ± 0.065§
Lung	0.0486 ± 0.0227	0.0497 ± 0.0096	0.0491 ± 0.0248	0.099 ± 0.140	0.0183 ± 0.0072
Liver	0.836 ± 0.086‡	1.185 ± 0.155	0.853 ± 0.565	0.899 ± 0.314	0.470 ± 0.189†
Kidney	0.241 ± 0.031	0.204 ± 0.0510	0.191 ± 0.111	0.209 ± 0.144	0.101 ± 0.051
Brain	0.0157 ± 0.0013	0.0207 ± 0.0057	0.0392 ± 0.0233	0.067 ± 0.049	0.0155 ± 0.0057
Bone	0.152 ± 0.032	0.153 ± 0.080	0.106 ± 0.074	0.235 ± 0.168	0.314 ± 0.133
Muscle	0.0132 ± 0.0024	0.0202 ± 0.0071	0.0314 ± 0.0224	0.031 ± 0.013	0.0110 ± 0.0060

\*Pretreated with etomoxir (40 mg/kg intraperitoneally) 2 h before.

†P < 0.02 vs. <sup>18</sup>F-FTO control fasted rats at 120 min.

‡P < 0.02 vs. <sup>18</sup>F-FTO control fasted rats at 30 min.

§P < 0.0005 vs. <sup>18</sup>F-FTO control fasted rats at 120 min.

Data are presented as mean ± SD.

<sup>18</sup>F-FTO increased from 30 to 120 min after injection, evidencing ongoing defluorination, similar to that of <sup>18</sup>F-FTP.

In fasted rats, myocardial uptake of <sup>18</sup>F-FTO was similar to that of <sup>18</sup>F-FTP at 30 min after injection (Table 1). At 2 h, myocardial uptake of <sup>18</sup>F-FTO was maintained, whereas <sup>18</sup>F-FTP uptake in the heart was 82% reduced. Hepatic clearance was faster for <sup>18</sup>F-FTP than for <sup>18</sup>F-FTO. Bone uptake for the 2 tracers was comparable at 120 min, suggesting that their defluorination rates in rats were equivalent.

Heart-to-organ ratios for <sup>18</sup>F-FTO and <sup>18</sup>F-FTP at 120 min after administration of tracers are shown in Figure 3. Heart-to-blood, heart-to-lung, and heart-to-liver ratios for <sup>18</sup>F-FTO were 4-, 4.8-, and 3.4-fold higher, respectively, than for <sup>18</sup>F-FTP.

Folch-type analysis of tissue extracts showed that <sup>18</sup>F-FTO is metabolized predominantly to protein-bound species in control hearts (Table 2), consistent with previous reports for <sup>18</sup>F-FTP (14) and <sup>18</sup>F-FTHA (16). At 30 min, the protein-bound fraction of radioactivity was significantly higher for <sup>18</sup>F-FTO (~90%) than for <sup>18</sup>F-FTP (~60%) (P < 0.05). Pretreatment of rats with etomoxir caused a dramatic shift from protein-bound species (>90%) to organic-soluble species (>65%) for <sup>18</sup>F-FTO at 30 min (Fig. 4), demonstrating the dependence of the formation of protein-bound metabolites on CPT-I dependent FAO. At 120 min, protein-bound, aqueous, and organic fractions in the liver were similar for <sup>18</sup>F-FTO and <sup>18</sup>F-FTP, but <sup>18</sup>F-FTO showed a 60% higher (P < 0.01) protein-bound fraction in the skeletal muscle than did <sup>18</sup>F-FTP (Table 2). Both organic and aqueous fractions were higher for <sup>18</sup>F-FTP than for <sup>18</sup>F-FTO in the skeletal muscle. The balance of non-protein-bound radioactivity for <sup>18</sup>F-FTO was split nearly evenly between aqueous and organic fractions as unidentified metabolites, whereas for <sup>18</sup>F-FTP, a larger fraction was found in the organic fraction. Thus, the data suggested that metabolic incorporation of the oleate analog <sup>18</sup>F-FTO into

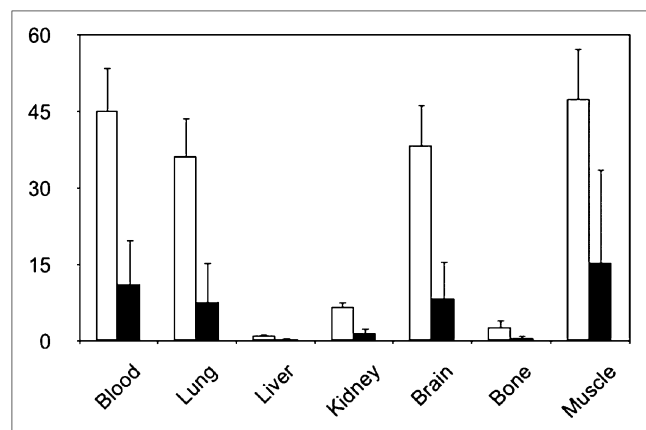


**FIGURE 3.** Heart-to-organ ratios for <sup>18</sup>F-FTO (open bars) and <sup>18</sup>F-FTP (filled bars) in fasted rats at 2 h after administration of radiotracers (n = 6, both groups). All <sup>18</sup>F-FTO values are statistically higher than <sup>18</sup>F-FTP values (P < 0.05).

**TABLE 2.** Distribution of  $^{18}\text{F}$  Radioactivity (% of Total) in Aqueous, Organic, and Pellet Fractions After Folch-Type Extraction of Tissues

Tracer	<i>n</i>	Time after injection (min)	Tissue	Aqueous (%)	Organic (%)	Pellet (%)
$^{18}\text{F}$ -FTO	6	30	Heart	3.3 ± 1.0	5.3 ± 1.3	91.4 ± 2.3
$^{18}\text{F}$ -FTP	6	30	Heart	2.6 ± 1.0	38.6 ± 19.0*	58.8 ± 19.2*
$^{18}\text{F}$ -FTO	6	120	Heart	1.8 ± 0.8	10.4 ± 1.8	87.7 ± 2.1
			Liver	5.6 ± 1.1	23.4 ± 3.1	70.9 ± 2.9
			Muscle	8.4 ± 0.1	11.7 ± 1.0	79.9 ± 1.1
$^{18}\text{F}$ -FTP	6	120	Heart	4.2 ± 1.3	18.8 ± 10.8	76.9 ± 10.8
			Liver	5.3 ± 0.9	31.4 ± 9.8	63.3 ± 9.3
			Muscle	16.2 ± 4.6*	34.0 ± 12.4*	49.8 ± 16.9*

\* $P < 0.01$  vs.  $^{18}\text{F}$ -FTO for same tissue, fraction, and time point. Rats were fasted overnight.

mitochondrial proteins of skeletal muscle appears to be similar to that shown in the heart (80–90%), whereas mitochondrial trapping of  $^{18}\text{F}$ -FTP represents approximately one half of its metabolic fate.

### Small-Animal PET Studies in Rats

A preliminary small-animal PET study was performed using  $^{18}\text{F}$ -FTO and  $^{18}\text{F}$ -FTP in separate groups of fasted rats (Fig. 5). Early dynamic images showed rapid blood clearance of both tracers to low radioactivity concentrations within 2 min after injection. Likewise, lung clearance was rapid, providing low background to the heart by 2 min after injection. The predominant hepatic uptake of the 2 fatty acid analogs peaked at 5 min after injection, followed by slow clearance. Myocardial uptake plateaued at about 10 min for both radiotracers, remaining nearly constant for  $^{18}\text{F}$ -FTO, whereas more pronounced myocardial clearance was observed for  $^{18}\text{F}$ -FTP. In the 2 rats studied, myo-

cardial uptake of  $^{18}\text{F}$ -FTO, expressed as standardized uptake value, was higher than that for  $^{18}\text{F}$ -FTP. This observation could not be explained by higher arterial concentrations of  $^{18}\text{F}$ -FTO: integrations of the blood pool curves over 0–2 min, when metabolites should not have a significant impact, were essentially the same for  $^{18}\text{F}$ -FTO and  $^{18}\text{F}$ -FTP. Whole-body images acquired at 55–115 min after injection demonstrated superior myocardial imaging characteristics of  $^{18}\text{F}$ -FTO consistent with the biodistribution data (Fig. 5). Myocardial uptake relative to liver and bone was markedly lower for  $^{18}\text{F}$ -FTP. Bone uptake in the ribs was seen with both radiotracers, evidencing *in vivo* defluorination in the rat.

### DISCUSSION

FAO is the major energy-providing process in the heart, liver, and skeletal muscle. Because disturbances of FAO are associated with many cardiovascular, gastrointestinal, oncologic, neurologic, and metabolic disorders, a non-invasive imaging method has great potential to affect the clinical care of patients. An imaging method would be of great value for monitoring disease progression and the effects of a growing number of drug therapies aimed at modifying FAO rates (23–25). The current study extends our previous work with thia-substituted fatty acid analogs (12,14,16) to develop an  $^{18}\text{F}$ -labeled fatty acid molecule that can serve as a metabolically trapped, general-purpose probe for PET of FAO in humans.

To date, nearly all the PET studies of fatty acid metabolism have been performed using  $^{11}\text{C}$ - or  $^{18}\text{F}$ -labeled saturated fatty acid analogs such as  $^{11}\text{C}$ -palmitate and  $^{18}\text{F}$ -labeled palmitate. The early studies of Knust et al. (26) showed that in mice  $^{18}\text{F}$ -fluoro fatty acids distribute in a manner similar to palmitate. As is the case for  $^{11}\text{C}$ -palmitate, the FAO rate must be derived from the clearance kinetics of the radiolabel, requiring various assumptions and complex tracer kinetic modeling approaches (27). The  $^{11}\text{C}$ -palmitate modeling method has not been validated in ischemic myocardium because of an elevated and variable level of backdiffusion of nonmetabolized radiotracer that confounds the clearance of labeled catabolite (27,28).

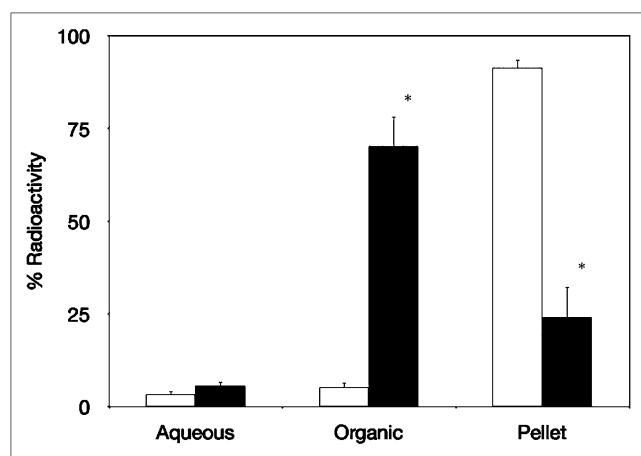


**FIGURE 4.** Effect of CPT-I inhibitor etomoxir (40 mg/kg intraperitoneal pretreatment 2 h before) on  $^{18}\text{F}$  radioactivity distribution in Folch-type extractions of rat hearts analyzed at 30 min after intravenous administration of  $^{18}\text{F}$ -FTO (control group,  $n = 6$ ; etomoxir group,  $n = 4$ ). Rats were fasted overnight. Statistical significance of etomoxir-induced changes: \* $P < 0.02$  vs. control.

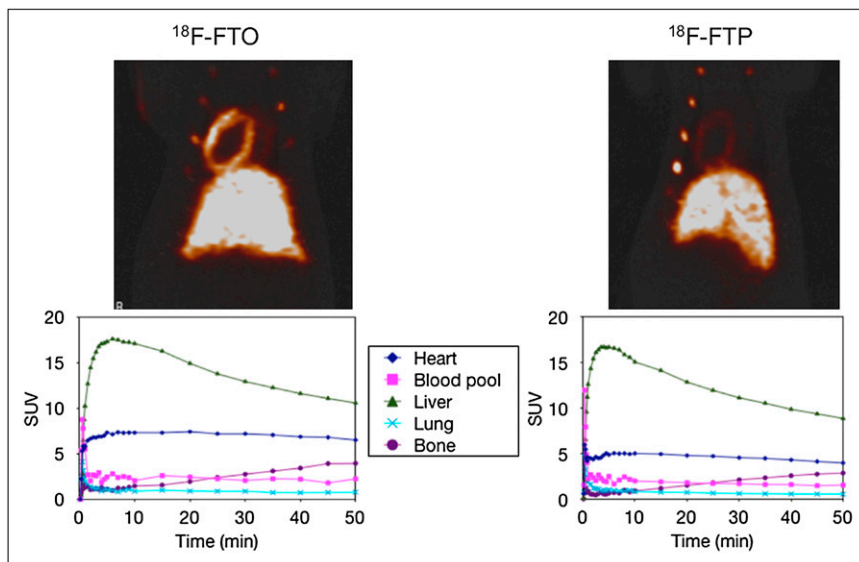


**FIGURE 5.** Early time-activity curves for  $^{18}\text{F}$ -FTO and  $^{18}\text{F}$ -FTP in rat heart (left ventricle), liver, lung, bone (rib), and blood pool and PET thoracic images acquired at 55–115 min after administration. Heart, bone, and liver uptake is evident on PET images. Higher heart-to-liver radioactivity concentration ratio was seen with  $^{18}\text{F}$ -FTO. Blood-pool data were not corrected for spillover effect from myocardium.

Various branched-chain fatty acid analogs have been developed as metabolically retained probes (29,30), but they are poorly accepted for transport into the mitochondrion through CPT-I (31), rendering them sensitive for the indication of extramitochondrial lipid incorporation processes but not sensitive for the indication of FAO. Our approach of sulfur substitution (16) followed earlier work with larger heteroatom substituents (32). It was established that the sulfur substitution greatly diminishes the incorporation of fatty acids into complex lipids (33), rendering its kinetics more specific to mitochondrial metabolism.  $^{18}\text{F}$ -FTHA, a 6-thia analog, was shown to be sensitive to CPT-I inhibition (16), but later studies indicated FAO-independent retention of radiotracer in hypoxic myocardium (19). Later, the 4-thia analog  $^{18}\text{F}$ -FTP was found to correlate well with FAO rates in isolated rat hearts in normoxic and hypoxic conditions (12,14). However, both  $^{18}\text{F}$ -FTHA (16) and  $^{18}\text{F}$ -FTP (14) showed significant clearance from rodent myocardium between an early peak (<10 min) and 2 h after administration. Slow but appreciable myocardial clearance was also observed in humans with  $^{18}\text{F}$ -FTHA (34), although  $^{18}\text{F}$ -FTP was well retained in healthy swine myocardium (14).

This is the first report of a positron-emitter labeled oleate analog. The 4-thia oleate analog  $^{18}\text{F}$ -FTO was synthesized in practical yield by analogy with  $^{18}\text{F}$ -FTP. Because of the presence of the *cis* double bond, the synthesis of the labeling precursor of  $^{18}\text{F}$ -FTO involved multiple steps but was straightforward. Because both  $^{18}\text{F}$ -FTO and  $^{18}\text{F}$ -FTP share the 4-thia substitution, any differences in their biodistributions and biochemical handling can be attributed to differences in chain length and unsaturation. The initial myocardial uptake of  $^{18}\text{F}$ -FTO was similar to that of  $^{18}\text{F}$ -FTP, but myocardial retention was dramatically increased. Although there was no evidence of clearance of  $^{18}\text{F}$ -FTO from the rat myocardium out to 2 h after injection, there was approximately 80% clearance of  $^{18}\text{F}$ -FTP from 30 to 120 min. The reasons for the higher myocardial retention of

$^{18}\text{F}$ -FTO are not clear. There was evidence in the Folch-type tissue-extraction measurements that  $^{18}\text{F}$ -FTO had a higher specificity to indicate mitochondrial FAO in the heart than did  $^{18}\text{F}$ -FTP. The protein-bound fraction of  $^{18}\text{F}$  radioactivity of 4-thia (18) and 6-thia (20) fatty acid analogs indicates the accumulation of FAO-dependent metabolites in the tissue, as supported by profound decreases of this fraction with CPT-I inhibition. This fraction decreased from 80% to 45% for  $^{18}\text{F}$ -FTP in rat heart (30 min after injection) under control and CPT-I-inhibited conditions, respectively (18). In contrast, the protein-bound fraction in the rat heart for  $^{18}\text{F}$ -FTO decreased from 90% to 25% under control and CPT-I-inhibited conditions, respectively (Fig. 4). However, decreases in myocardial uptake caused by CPT-I inhibition (~80%) at 30 min after injection were found to be equivalent for  $^{18}\text{F}$ -FTO and  $^{18}\text{F}$ -FTP (18). Both  $^{18}\text{F}$ -FTO and  $^{18}\text{F}$ -FTP appear to be highly specific probes for the indication of FAO in the heart. However, the slower myocardial clearance and 3- to 4-fold higher heart-to-blood, heart-to-lung, and heart-to-liver radioactivity concentration ratios favor  $^{18}\text{F}$ -FTO over  $^{18}\text{F}$ -FTP for heart imaging applications.

With regard to skeletal muscle, our measurements at 120 min after injection showed  $^{18}\text{F}$ -FTO to have a significantly higher protein-bound fraction relative to  $^{18}\text{F}$ -FTP (Table 2), indicating that  $^{18}\text{F}$ -FTO may have better utility for the evaluation of FAO in skeletal muscle. Previous work with  $^{18}\text{F}$ -FTHA in pigs had shown the 6-thia analog to be poorly taken up into skeletal muscle mitochondria (35). Taken together with the results of the present study, the approximate distribution of  $^{18}\text{F}$ -FTHA,  $^{18}\text{F}$ -FTP, and  $^{18}\text{F}$ -FTO to the protein-bound mitochondrial fraction of control skeletal muscle is 36%, 50%, and 80%, respectively. Thus, the results indicate that  $^{18}\text{F}$ -FTO kinetics are sufficiently specific in skeletal muscle to warrant further evaluation of  $^{18}\text{F}$ -FTO as an FAO probe for monitoring of FAO in metabolic disorders that involve skeletal muscle.

The suggested enhancement of specificity of  $^{18}\text{F}$ -FTO relative to  $^{18}\text{F}$ -FTP and  $^{18}\text{F}$ -FTHA for the indication of FAO in skeletal muscle has some support from previous studies of oleate and palmitate metabolism. A whole-body metabolism study in humans showed that dietary  $^{13}\text{C}$ -oleate was preferentially oxidized relative to dietary  $^{13}\text{C}$ -palmitate (22). Because skeletal muscle is the major consumer of fatty acids in the body, this study implied that skeletal muscle preferentially oxidized oleate relative to palmitate. Likewise, a human feeding study in which the ratio of polyunsaturated to saturated fatty acids in the diet was altered also suggested that polyunsaturated fatty acids are more highly oxidized than are saturated fatty acids (36).

Heart and skeletal muscle uptake of  $^{18}\text{F}$ -FTO was found to be the same in fed and fasted rats. This does not imply equivalent FAO rates in heart and muscle in the different feeding conditions. Radiotracer uptake is a measure of the fraction of dose taken up per gram of tissue. Taking into consideration that plasma concentrations of nonesterified fatty acids are 2.2-fold higher in the fasted state than in the fed state in the same experimental conditions (14), equivalent uptake is consistent with higher FAO rates in fasted animals in heart and skeletal muscle.

The liver is a predominant organ of uptake for  $^{18}\text{F}$ -FTO, consistent with previously developed fatty acid radiotracers. Folch-type extraction analysis of livers from rats administered  $^{18}\text{F}$ -FTO showed that  $70.9 \pm 2.9\%$  of the trapped  $^{18}\text{F}$  radioactivity was in the form of protein-bound metabolites at 2 h after injection, indicating that  $^{18}\text{F}$ -FTO may be useful for the evaluation of hepatic FAO rates. In comparison,  $^{18}\text{F}$ -FTHA showed  $57.5 \pm 1.9\%$  protein-bound metabolites at 10 min after injection (16), and  $^{18}\text{F}$ -FTP was in between ( $63.3 \pm 9.3\%$  at 2 h after injection). Notably, the liver uptake of  $^{18}\text{F}$ -FTO was significantly lower in fed rats than in fasted rats ( $0.836 \pm 0.086\%$  vs.  $1.185 \pm 0.155\%$  dose kg/g at 30 min after injection), consistent with lower hepatic FAO rates in the fed state.  $^{18}\text{F}$ -FTP lacked this sensitivity ( $1.24 \pm 0.44\%$  vs.  $1.15 \pm 0.16\%$  dose kg/g) (14). The lack of a response of liver uptake of  $^{18}\text{F}$ -FTO to the CPT-I inhibitor etomoxir at 30 min after injection likely reflects the presence of uptake and oxidation mechanisms that are CPT-I-independent in the liver, such as peroxisomal FAO. Etomoxir was found to paradoxically stimulate palmitate oxidation in rat liver homogenates through a peroxisome-dependent pathway (37). The PET-measured hepatic concentrations of the thia fatty acid analogs are relevant to hepatic fatty acid uptake and oxidation, with  $^{18}\text{F}$ -FTO being the most specific to date for indicating FAO.

The in vivo defluorination of  $\omega$ -labeled, non- $\beta$ -oxidizable  $^{18}\text{F}$ -fluoro-fatty acids is known to be problematic in rodents (38) but has not been observed to be a problem in pigs or humans (14). Because the synthesis of labeling precursor is more straightforward for labeling at the  $\omega$ -position, we developed  $^{18}\text{F}$ -FTO as the first oleate analog. Should defluorination of  $^{18}\text{F}$ -FTO be found in subsequent studies in large animals and humans, an  $\omega$ -3-labeled

analog will be developed to stabilize the  $^{18}\text{F}$  radiolabel (38).

## CONCLUSION

A practical and high-purity synthesis of the oleate analog  $^{18}\text{F}$ -FTO was developed.  $^{18}\text{F}$ -FTO exhibited 3- to 4-fold higher heart-to-background tissue radioactivity concentration ratios, resulting from higher myocardial retention relative to  $^{18}\text{F}$ -FTP.  $^{18}\text{F}$ -FTO uptake by the heart was approximately 80% reduced by pretreatment of rats with the CPT-I inhibitor etomoxir. Folch-type extraction analyses showed 70–90% protein-bound fractions in the heart, liver, and skeletal muscle, consistent with the high trafficking of  $^{18}\text{F}$ -FTO to the mitochondrion with subsequent metabolism to protein-bound species. Small-animal PET images of  $^{18}\text{F}$ -FTO accumulation in the rat myocardium were clearly superior to those of  $^{18}\text{F}$ -FTP.  $^{18}\text{F}$ -FTO has been shown to be a promising metabolically trapped FAO probe that improves on the myocardial imaging characteristics of  $^{18}\text{F}$ -FTP and warrants further evaluation.

## ACKNOWLEDGMENTS

We thank Aditya Bansal for his assistance. We acknowledge the support of the NIH (grants R01 HL-63371 and R01 CA108620). Dr. Timothy DeGrado is a shareholder of Tracera, LLC.

## REFERENCES

1. Wang W, Lopaschuk GD. Metabolic therapy for the treatment of ischemic heart disease: reality and expectations. *Expert Rev Cardiovasc Ther.* 2007;5:1123–1134.
2. Fragasso G, Spoladore R, Bassanelli G, et al. New directions in the treatment of heart failure: targeting free fatty acid oxidation. *Curr Heart Fail Rep.* 2007;4:236–242.
3. Tuunanen H, Kuusisto J, Toikka J, et al. Myocardial perfusion, oxidative metabolism, and free fatty acid uptake in patients with hypertrophic cardiomyopathy attributable to the Asp175Asn mutation in the  $\alpha$ -tropomyosin gene: a positron emission tomography study. *J Nucl Cardiol.* 2007;14:354–365.
4. Liu Y. Fatty acid oxidation is a dominant bioenergetic pathway in prostate cancer. *Prostate Cancer Prostatic Dis.* 2006;9:230–234.
5. de la Monte SM, Wands JR. Alzheimer's disease is type 3 diabetes-evidence reviewed. *J Diabetes Sci Technol.* 2008;2:1101–1113.
6. You M, Crabb DW. Recent advances in alcoholic liver disease II: minireview—molecular mechanisms of alcoholic fatty liver. *Am J Physiol Gastrointest Liver Physiol.* 2004;287:G1–G6.
7. Kotronen A, Seppala-Lindroos A, Vehkavaara S, et al. Liver fat and lipid oxidation in humans. *Liver Int.* 2009;29:1439–1446.
8. Young ME, Guthrie PH, Razeghi P, et al. Impaired long-chain fatty acid oxidation and contractile dysfunction in the obese Zucker rat heart. *Diabetes.* 2002;51:2587–2595.
9. Bugger H, Abel ED. Molecular mechanisms for myocardial mitochondrial dysfunction in the metabolic syndrome. *Clin Sci (Lond).* 2008;114:195–210.
10. Leonhardt M, Langhans W. Fatty acid oxidation and control of food intake. *Physiol Behav.* 2004;83:645–651.
11. Barsotti A, Giannoni A, Di Napoli P, Emdin M. Energy metabolism in the normal and in the diabetic heart. *Curr Pharm Des.* 2009;15:836–840.
12. DeGrado TR, Kitapci MT, Wang S, Ying J, Lopaschuk GD. Validation of  $^{18}\text{F}$ -fluoro-4-thia-palmitate as a PET probe for myocardial fatty acid oxidation: effects of hypoxia and composition of exogenous fatty acids. *J Nucl Med.* 2006;47:173–181.
13. Wallhaus TR, Taylor M, DeGrado TR, et al. Myocardial free fatty acid and glucose use after carvedilol treatment in patients with congestive heart failure. *Circulation.* 2001;103:2441–2446.

14. DeGrado TR, Wang S, Holden JE, Nickles RJ, Taylor M, Stone CK. Synthesis and preliminary evaluation of  $^{18}\text{F}$ -labeled 4-thia palmitate as a PET tracer of myocardial fatty acid oxidation. *Nucl Med Biol.* 2000;27:221–231.
15. Renstrom B, Rommelfanger S, Stone CK, et al. Comparison of fatty acid tracers FTHA and BMIPP during myocardial ischemia and hypoxia. *J Nucl Med.* 1998;39:1684–1689.
16. DeGrado TR, Coenen HH, Stocklin G. 14(R,S)-[ $^{18}\text{F}$ ]fluoro-6-thia-heptadecanoic acid (FTHA): evaluation in mouse of a new probe of myocardial utilization of long chain fatty acids. *J Nucl Med.* 1991;32:1888–1896.
17. Stone CK, Pooley RA, DeGrado TR, et al. Myocardial uptake of the fatty acid analog 14-fluorine-18-fluoro-6-thia-heptadecanoic acid in comparison to  $\beta$ -oxidation rates by tritiated palmitate. *J Nucl Med.* 1998;39:1690–1696.
18. Wisneski JA, Gertz EW, Neese RA, Mayr M. Myocardial metabolism of free fatty acids: studies with  $^{14}\text{C}$ -labeled substrates in humans. *J Clin Invest.* 1987;79:359–366.
19. Kanaley JA, Shadid S, Sheehan MT, Guo Z, Jensen MD. Relationship between plasma free fatty acid, intramyocellular triglycerides and long-chain acylcarnitines in resting humans. *J Physiol.* 2009;587:5939–5950.
20. Bergouignan A, Momken I, Schoeller DA, Simon C, Blanc S. Metabolic fate of saturated and monounsaturated dietary fats: the Mediterranean diet revisited from epidemiological evidence to cellular mechanisms. *Prog Lipid Res.* 2009;48:128–147.
21. Bergouignan A, Trudel G, Simon C, et al. Physical inactivity differentially alters dietary oleate and palmitate trafficking. *Diabetes.* 2009;58:367–376.
22. DeLany JP, Windhauser MM, Champagne CM, Bray GA. Differential oxidation of individual dietary fatty acids in humans. *Am J Clin Nutr.* 2000;72:905–911.
23. Folmes CD, Clanachan AS, Lopaschuk GD. Fatty acid oxidation inhibitors in the management of chronic complications of atherosclerosis. *Curr Atheroscler Rep.* 2005;7:63–70.
24. Di Napoli P, Taccardi AA, Barsotti A. Long term cardioprotective action of trimetazidine and potential effect on the inflammatory process in patients with ischaemic dilated cardiomyopathy. *Heart.* 2005;91:161–165.
25. Wambolt RB, Lopaschuk GD, Brownsey RW, Allard MF. Dichloroacetate improves posts ischemic function of hypertrophied rat hearts. *J Am Coll Cardiol.* 2000;36:1378–1385.
26. Knust EJ, Kupfermagel C, Stocklin G. Long-chain F-18 fatty acids for the study of regional metabolism in heart and liver; odd-even effects of metabolism in mice. *J Nucl Med.* 1979;20:1170–1175.
27. Bergmann SR, Weinheimer CJ, Markham J, Herrero P. Quantitation of myocardial fatty acid metabolism using PET. *J Nucl Med.* 1996;37:1723–1730.
28. Fox KA, Abendschein DR, Ambos HD, Sobel BE, Bergmann SR. Efflux of metabolized and nonmetabolized fatty acid from canine myocardium: implications for quantifying myocardial metabolism tomographically. *Circ Res.* 1985;57:232–243.
29. Livni E, Elmaleh DR, Barlai-Kovach MM, Goodman MM, Knapp FF Jr., Strauss HW. Radioiodinated  $\beta$ -methyl phenyl fatty acids as potential tracers for myocardial imaging and metabolism. *Eur Heart J.* 1985;(6 suppl B): 85–89.
30. Livni E, Elmaleh DR, Levy S, Brownell GL, Strauss WH. Beta-methyl[1- $^{11}\text{C}$ ] heptadecanoic acid: a new myocardial metabolic tracer for positron emission tomography. *J Nucl Med.* 1982;23:169–175.
31. DeGrado TR, Holden JE, Ng CK, Raffel DM, Gatley SJ. Beta-methyl-15-p-iodophenylpentadecanoic acid metabolism and kinetics in the isolated rat heart. *Eur J Nucl Med.* 1989;15:78–80.
32. Goodman MM, Knapp FF Jr, Callahan AP, Ferren LA. Synthesis and biological evaluation of 17- $^{131}\text{I}$ iodo-9-telluraheptadecanoic acid, a potential imaging agent. *J Med Chem.* 1982;25:613–618.
33. Skrede S, Sorensen HN, Larsen LN, et al. Thia fatty acids, metabolism and metabolic effects. *Biochim Biophys Acta.* 1997;1344:115–131.
34. Ebert A, Herzog H, Stocklin GL, et al. Kinetics of 14(R,S)-fluorine-18-fluoro-6-thia-heptadecanoic acid in normal human hearts at rest, during exercise and after dipyridamole injection. *J Nucl Med.* 1994;35:51–56.
35. Takala TO, Nuutila P, Pulkki K, et al. 14(R,S)-[ $^{18}\text{F}$ ]Fluoro-6-thia-heptadecanoic acid as a tracer of free fatty acid uptake and oxidation in myocardium and skeletal muscle. *Eur J Nucl Med Mol Imaging.* 2002;29:1617–1622.
36. Jones PJ, Schoeller DA. Polyunsaturated:saturated ratio of diet fat influences energy substrate utilization in the human. *Metabolism.* 1988;37:145–151.
37. Noland RC, Woodlief TL, Whitfield BR, et al. Peroxisomal-mitochondrial oxidation in a rodent model of obesity-associated insulin resistance. *Am J Physiol Endocrinol Metab.* 2007;293:E986–E1001.
38. DeGrado TR, Moka DC. Non-beta-oxidizable omega-[ $^{18}\text{F}$ ]fluoro long chain fatty acid analogs show cytochrome P-450-mediated defluorination: implications for the design of PET tracers of myocardial fatty acid utilization. *Int J Rad Appl Instrum B.* 1992;19:389–397.